*Atmosfera (1997)*, **10**, *pp. 101-123*

# Effects of the autumn-winter meteorology upon the surface heat loss in the Northern Gulf of California

A. C. REYES* and M. F. LAVIN

*Centro de Investigación Científica y de Educación Superior de Ensenada, Ensenada B. C., México*

(Manuscript received February 14, 1996; accepted in final form August 14, 1996)

RESUMEN

Datos meteorológicos costeros de cinco períodos otoño-invierno (1982/83 a 1986/87), son usados para describir la meteorología (y su variabilidad) que afecta la región Norte del Golfo de California, con especial atención a los eventos con viento intenso que son considerados los causantes de las principales pérdidas de calor durante esta temporada. Los períodos otoño-invierno de 1982/83 y 1986/87 muestran anomalías en la humedad relativa (en cada uno de estos períodos ocurrió un evento ENOS): El primero tuvo la mayor (63%) y el segundo la menor (43%). También, la mayor rapidez media del viento se registró en 1982/83. Las diferencias entre estos dos períodos podrían ser explicadas por las trayectorias seguidas por las masas de aire que llegan a la región: en 1982/83, la dirección del viento indica una mayor influencia oceánica del Pacífico que la observada en 1986/87. Flujos de calor fueron calculados con el modelo de una columna de agua bien mezclada de 30 m de profundidad la cual representa la región somera de la cabeza del golfo, donde ocurre la formación de masas de agua durante el otoño-invierno. El modelo usa datos meteorológicos y el valor del flujo lateral de calor obtenido mediante un balance de calor. La mayor parte de la pérdida neta de calor (67%) ocurren durante períodos con viento intenso ($\sim$7 $ms^{-1}$, principalmente del NO) y baja humedad relativa ($\sim$56 %), que varían entre 1 y 15 días. El flujo de calor latente produce la mayor pérdida de calor, con aproximadamente 67% del total. Las dos variables más importantes para los flujos de calor, rapidez de viento y humedad relativa, tienen una variabilidad bimodal, que a su vez modula el flujo de calor latente: La rapidez del viento tiene máximos en noviembre y enero, mientras que la humedad relativa tiene máximos en diciembre y febrero. En el promedio la mayor pérdida de calor ocurre en noviembre, aun cuando los eventos más fuertes de pérdida de calor ocurren en noviembre y marzo. La variabilidad meteorológica interanual tiene un efecto notable sobre los flujos de calor: la menor pérdida de calor (-2 $Wm^{-2}$) ocurrió en el otoño-invierno de 1982/83, mientras que la mayor pérdida (-30 $Wm^{-2}$) ocurrió en el período de 1986/87.

ABSTRACT

Coastal meteorological data of five autumn-winter periods (1982/83 to 1986/87), are used to describe the meteorology (and its variability) affecting the Northern Gulf of California, focusing on the strong wind events which have been proposed to cause most of the autumn-winter heat loss. The 1982/83 and 1986/87 autumn-winter periods were found to have anomalous relative humidity (an ENSO event was in progress in both periods): the first one had the highest ($\sim$63%) and the second the lowest ($\sim$43%) humidity. Also, the highest mean wind speeds were recorded in 1982/83. The differences between these two periods could be due to the pathway followed by the air masses: in 1982/83, the wind direction suggests a more oceanic influence from the Pacific than in 1986/87. The heat fluxes were calculated with a 30 m-deep well-mixed model representing the shallow region at the head of the

* Present address: Center for Coastal Physical Oceanography, Old Dominion University, 758 52nd Street. Norfolk VA, USA

gulf, where water-mass formation takes place in autumn-winter. The model is driven by the meteorological data and a lateral heat flux obtained by heat balance. Most of the net heat loss (67%) takes place during periods of strong winds ($\sim$7 $ms^{-1}$, mostly NW) and low relative humidity ($\sim$56%), lasting from 1 to 15 days. Latent heat flux is the main surface heat loss, accounting for about 67% of the total. The two most important variables for the heat fluxes, wind speed and humidity, have a bimonthly variability, which in turn modulate the latent heat flux: wind speed has maxima in November and January, while humidity has maxima in December and February. In the average the highest net heat loss occurs in November, although the strongest heat-loss events occur in October and March. The interannual meteorological variability has a noticeable effect upon the heat flux: the lowest heat loss (-2 $Wm^{-2}$) occurred in the autumn-winter of 1982/83, while the highest occurred in that of 1986/87 (-30 $Wm^{-2}$).

## 1. Introduction

The Northern Gulf of California (henceforth NGC, Fig. 1), lies in the boundary between the tropical and the subtropical atmospheric circulation regimes, between 29°N and 31.6°N. It is a tidal shallow sea, with $\sim$70% of its area less than 200 m deep, and therefore it responds rather quickly to the spectrum of meteorological variability. At the head of the gulf, complete vertical mixing exists from the shore to about the 30 m isobath in summer and about 100 m in winter (Organista, 1987; Martínez-Sepúlveda, 1994; Argote *et al.*, 1995). The NGC is surrounded by deserts and is characterized by marine and atmospheric isolation; the former owing to the midriff archipelago among which lie several sills, which restrict communication with the rest of the gulf to above about 400 m. From the atmospheric point of view, there are mountain ridges on both sides of the gulf, and those in the peninsula hinder the influence of the lower layers of the atmosphere over the Pacific Ocean upon the NGC; therefore the climate in this region is more Mediterranean than marine.

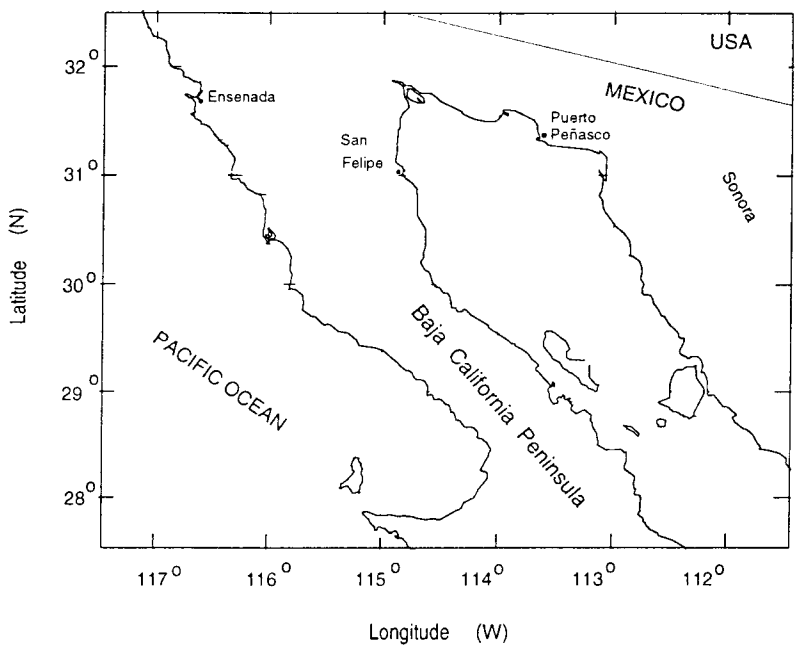


Figure 1. The Northern Gulf of California, and location of the coastal meteorological stations at San Felipe and Puerto Peñasco.

The climate over the gulf presents two clearly differentiated seasons: a mid-latitude winter and a subtropical summer (Roden, 1958; García and Mosiño, 1966-67; Badan-Dangon *et al.*, 1991). During most of the year the NGC can be affected by mid-latitude air masses, and in summer it can also be affected by tropical events (Reyes *et al.*, 1984; Reyes and Rojo, 1985). Although the Gulf of California presents clear meteorological differences between the north and south regions (Reyes and Vogel, 1984), the spatial variation of the meteorological variables inside the NGC, and away from the coast, is not considered significant (Merrifield and Winant, 1989; Paden *et al.*, 1991; Badan-Dangon *et al.*, 1991).

During summer, the synoptic surface atmospheric circulation in the NGC is dominated by a low-pressure cell usually located over Arizona, which separates in a general sense the Pacific High and the high-pressure system that extends from the Bermuda to the Southeastern United States (Fig. 2a) (García and Mosiño, 1966; Reyes *et al.*, 1984), this low pressure favors the advection of tropical moisture up the gulf. Hales (1972) noticed that during summer the Gulf of California serves as a natural corridor for most of near surface moisture that reaches the SW United States. Recent studies agree with this description (Badan-Dangon *et al.*, 1991; Douglas *et al.*, 1994).

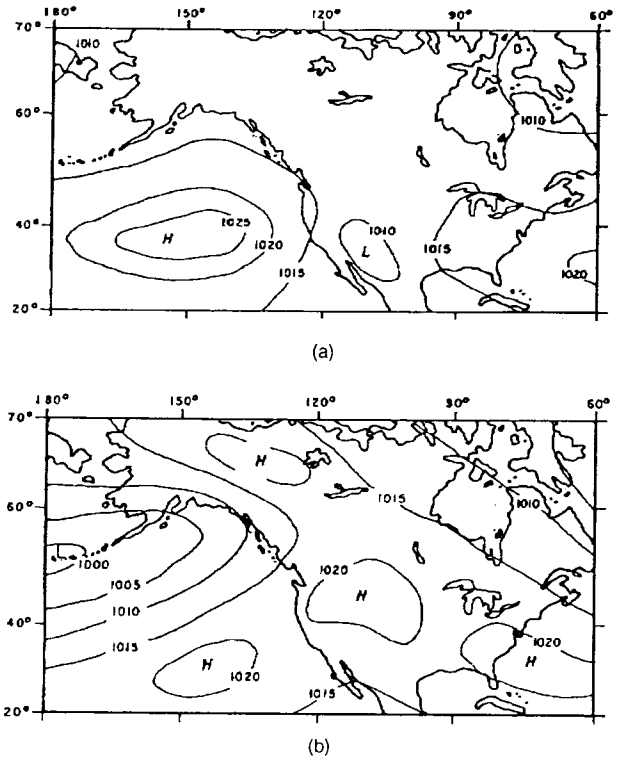


Figure 2. Typical synoptic distribution of surface atmospheric pressure (milibars) that affect the Gulf of California in (a) summer and (b) winter. Adapted from Igmanson and Wallace [1985].

In winter (Fig. 2b), as a consequence of the annual heating cycle, the northern central region of North America is characterized by an anticyclone which is an extension of the Bermuda high-pressure system, while the low pressure cell is displaced to the SE, over NW Mexico (Roden, 1958). The Pacific High is established offshore of the SW coast of the Unites States (Badan-Dangon *et al.*, 1991), and its position is frequently modified by the generation and eastward

displacement of cyclonic cells which give rise to the "rainy winter", characteristic of this area (Sorkina, 1963; Bailey, 1975; Zishka and Smith, 1980; Reyes and Rojo, 1985; Reyes *et al.*, 1984; Reyes and Vogel, 1984). Following the passage of those low-pressure systems, intense, cold NW winds, caused by a larger influence of the high pressure system over the SW United States, reach the NGC (Ives, 1962; Badan-Dangon *et al.* 1991; Reyes, 1993); this occurs as a series of episodes, 3 to 10 days long.

The net surface heat flux in the NGC has a pronounced seasonality, in addition to an annual heat gain by the sea (Lavin and Organista, 1988; Paden *et al.*, 1993; Castro *et al.*, 1994). During spring and summer, when there is a higher insolation and the dominant SE winds bring moist tropical air from the SE, the Gulf of California gains heat. In winter, the lower insolation and the greater atmospheric extratropical activity produce a net heat loss through the surface. This heat loss can cause the waters of the NGC to become vertically unstable, producing overturns and water-mass formation (Sverdrup, 1941), an important mechanism for the renewal of the waters of the NGC. Bray (1988) has proposed that this phenomenon takes place during the winter-time synoptic events described above. Although this has not been proved, the sea surface temperature (SST) in the NGC responds rapidly to air temperature fluctuations due to synoptic activity (Paden *et al.*, 1991).

Although the interannual variability of atmospheric conditions in the NGC has not been thoroughly investigated, there is some evidence relating it with ENSO events. Reyes and Rojo (1985) found that strong positive anomalies of the Austral Index (AI) coincide with greater precipitation at the northern region of the peninsula of Baja California. Positive anomalies of relative humidity in the NGC, apparently associated to ENSO events, have been documented by Organista (1987). Paden *et al.* (1993) have suggested that during ENSO, humidity over the gulf may be higher than normal, and that the seasonal cycle of relative humidity is attenuated.

In this paper we study the winter meteorological synoptic activity in the NGC, its interannual variability, and their effect upon heat losses through the surface of the sea. A future paper will discuss its effect upon water-mass formation.

## 2. Data

The data are daily means of hourly data taken from the Mexican Weather Service Observatory at San Felipe (31°N, 114.7°W, Fig. 1). The data covers the autumn-winter months (October to March) of 1982/83 to 1986/87. Regrettably, wind data from San Felipe is not available after March 1987. The variables used are: air temperature (°C), relative humidity (%), atmospheric pressure (mb), cloud cover (oktas) and wind velocity (m/s).

Although near surface atmospheric conditions over the NGC are considered almost homogeneous, the meteorological station at San Felipe is about 1 km inland, and the hourly data show enhanced diurnal fluctuations and lower wind speeds and humidities, when compared with data collected offshore. To quantify and correct for this effect, daily mean data sets from San Felipe were compared against simultaneous data from the better-situated meteorological stations at Puerto Peñasco (Fig. 1) and from three oceanographic surveys in the NGC (Table I). The wind speed and relative humidity have a mean ratio of 2.55 and 1.28 respectively (Reyes, 1993). The wind speed ratio is similar to that suggested by Badan-Dangon et al. (1991) for the same region, and to the more general results of Franklin and Blanton (1984). Only these two variables are modified because they present the largest differences and are the most influential in the heat flux calculations. Recent observations from an anchored meteorological buoy in the NGC, by the "Centro de Investigación Científica y de Educación Superior de Ensenada", support the mean ratio found for wind speed.

Table I. Data used to transform San Felipe wind velocity and humidity data to offshore conditions.

| Site/Cruise | Dates | Sampling |
|---|---|---|
| Puerto Peñasco | Jan 83 to Mar 83 | Hourly data |
| Puerto Peñasco | Oct 83 to Dec 83 | Hourly data |
| EP8612 | Dec 12 to Dec 14, 1986 | Semihourly data |
| DS8803 | Feb 25 to Mar 03, 1988 | Semihourly data |
| EP9001 | Jan 8 to Jan 29, 1990 | Semihourly data |

The seasonal thermal behavior of the Northern Gulf of California was obtained from the hydrographic data bank used by Castro *et al.* (1994). Sea surface temperature (SST) from water columns of 30 and 75 m, corresponding respectively to the depth of the permanently mixed coastal zone at the head of the gulf, and to the mixed layer depth in October, were used to obtain monthly averages, which were then adjusted by least squares to an annual signal. We shall denote these series of observed SST by $< T_{so} >_{30}$ and $< T_{so} >_{75}$, or simply $< T_{so} >$ :

$$< T_{so} >_{30} = 23.11 - 5.3799 \cos \omega t - 4.9236 \sin \omega t \tag{1}$$

$$< T_{so} >_{75} = 22.69 - 5.0938 \cos \omega t - 3.9302 \sin \omega t \tag{2}$$

where $t$ is Julian days, and $\omega$ is the frequency $2\pi/365$ days$^{-1}$

## 3. Model

The net heat flux ($Q_f$) across the surface is:

$$Q_f = Q_s + Q_e + Q_b + Q_h \tag{3}$$

where $Q_s$ is the solar short wave radiation, $Q_e$ is the latent heat flux, $Q_b$ is the long-wave radiation and $Q_h$ is the sensible heat flux. $Q_e$ and $Q_b$ are always negative (from the sea to the atmosphere), $Q_h$ can be positive or negative. The heat fluxes were calculated using the bulk aerodynamic formulas used by Castro *et al.* (1994).

The net heat flux across the surface ($Q_f$) depends on the meteorological data and on the sea surface temperature, i.e. $Q_f$(met., $T_s$). The SST data used for the calculation of the heat fluxes is critical. It is possible to use $< T_{so} >$, an average value from observations (Lavín and Organista, 1988; Castro *et al.*, 1994), to obtain a climatological estimate of the fluxes. However, this approach does not permit the study of interannual variability. In order to do this, given only the meteorological data, the heat conservation equation can be used to predict the temperature of a well-mixed column, which is the same as its SST ($T_{sp}$). From $T_{sp}$ and the meteorological data, $Q_f$ can be estimated.

For a water column of depth $h$, the heat conservation equation is:

$$\rho C p h A (dT/dt) = Q_f A + q \tag{4}$$

where $\rho = 1024$ kg m$^{-3}$ is the reference water density, Cp = 3996 kg$^{-1}$K$^{-1}$ is the specific heat of sea water, $A$ is the surface area of the water column (to be taken as unitary from here on), $T$ is the temperature, and $q$ is the advective heat flux (in Watts).

In the Gulf of California, $q$ is not negligible, and an estimate of its climatological seasonal cycle can be obtained by balancing heat (Castro *et al.*, 1994). Denoting by <> the several-year average of data of each day of the year, applying this operator to equation (4) and solving for $< q >$, one gets

$$< q >= \rho C_p h < dT/dt > - < Q_f > \tag{5}$$

The mean rate of temperature change $< dT/dt >$ was calculated from $< T_{so} >$, defined by (1) and (2), and $< Q_f >$ was approximated by $< Q_f(\text{met.}, < T_{so} >) >$, that is, the daily average of the Qf calculated from the actual daily-mean meteorological data and the daily value of $< T_{so} >$. Thus $< q >$ is specified in a daily basis.

Equation (4) can then be integrated in time steps of 1 day, starting from an initial temperature (30 of September) obtained from $< T_{so} >$. In step $n$, $Q_f$ is calculated from the meteorological data and the bulk formulae using $T_{sp}(n-1)$. The water temperature for day $n$ is

$$T_{sp}(n) = T_{sp}(n-1) + (Q_f + < q >)\Delta t/\rho C_p h) \tag{6}$$

where $\Delta t = 1$ day. This produces predicted time series of water temperature $T_{sp}(t)$ and all the heat fluxes in (3).

## 4. Autumn-winter atmospheric conditions

### *(a) Short time scale (events)*

From fall to winter the interaction between the Pacific High over the SW coast of the USA, and the displacement of low pressure cells along the northeast or southwest anticyclone edges determines the origin of the air masses that reach the NGC. Therefore fluctuations in wind, relative humidity and cloudiness in San Felipe are well correlated to atmospheric pressure variations (1984/85, example in Fig. 3). Two main atmospheric conditions are distinguishable, which depend on the relative position of the high and low pressure cells with respect to the NGC (Table II, Figs. 4 and 5): (a) Weak SE wind, high relative humidity and cloudiness, when the low pressure cell is to the W of the NGC and the anticyclone to the N or NE of the NGC, and (b) stronger NW wind, low relative humidity and cloudiness when the low pressure cell is to the E of the NGC and the anticyclone to the W or NW.

As an example, the succession of a high and a low pressure systems from February 19 to 25, 1985, and their effect on the meteorological conditions in San Felipe are shown in Figures 4 and 5. On February 19, with a high pressure system over Utah, a low pressure cell (not visible in the figure) approximates the NGC, therefore the wind at San Felipe is E-SE, carrying humidity and clouds. On February 20 the low has displaced the high, at San Felipe the wind is E-SE for the first half of the day and later becomes SE-S, hence both cloud cover and relative humidity first decrease and then increase. On February 21 the low passes over the NGC, and in San Felipe the relative humidity falls. On February 22 the low pressure system is over New Mexico and Texas while the high pressure influences the NW of the USA, resulting in clear skies and SE winds in San Felipe. On February 23 the high pressure (not visible) produces NW wind and clear skies. On February 24 the high is found again over Utah and the wind in San Felipe changes from NW to NE while the sky remains clear and the relative humidity falls. On February 25 the high pressure cell is over the Pacific, while isobars at the NGC show the incipient influence of warm tropical air.

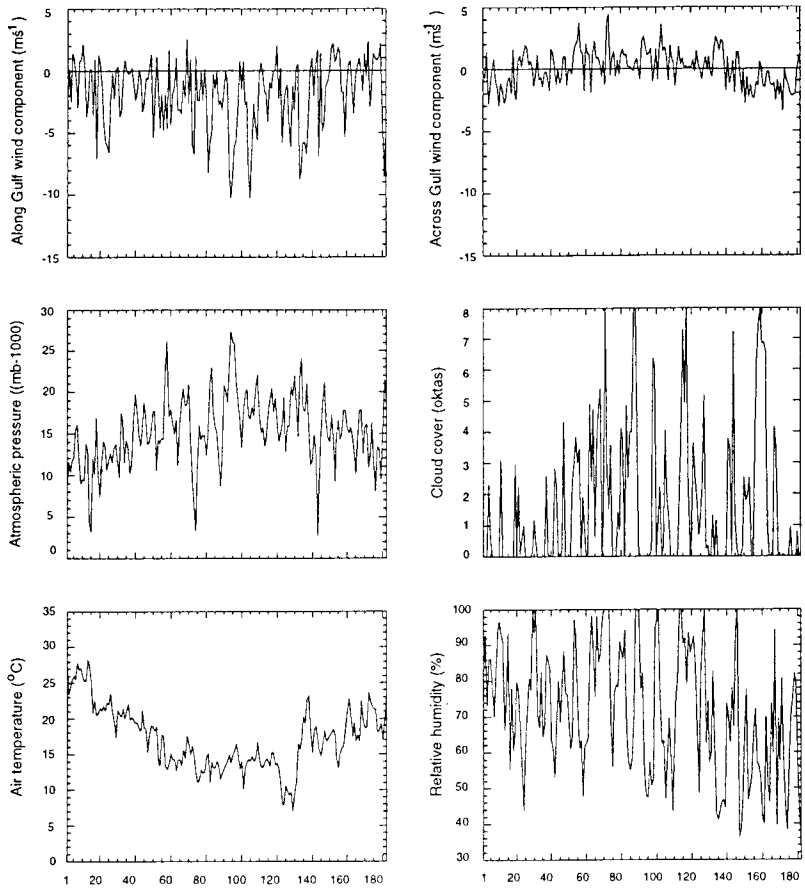


Figure 3. Daily meteorological data from San Felipe in the autumn-winter 1984/85, after convertion to offshore values (see text). Along and across Gulf winds positive towards 325° T and 55° T, respectively.

Table II. Mean meteorological parameters observed at San Felipe during the situations: a) The low pressure cell to the W of NGC and the anticyclone to the N or NE of the NGC. b) The low pressure cell to the E of the NGC and the anticyclone to the W or NW of the NGC.

| Case | Air T (°C) | H (%) | Air p (mb) | Cloud (okta) | Speed (m/s) | Along (m/s) | Across (m/s) |
|---|---|---|---|---|---|---|---|
| a) | 23.0 | 62.7 | 1012.7 | 1.5 | 4.0 | 1.0 | -1.53 |
| b) | 23.2 | 44.6 | 1017.5 | 1.0 | 8.4 | -7.9 | 0.51 |

We define "intense, or strong wind events" or simply "events", those from the NE to NW whose speed exceed 5.1 $ms^{-1}$ and whose along-gulf component is greater than 2.5 $ms^{-1}$. The mean characteristics of these events are presented in Table III. The average number of such events per month is about 4, their frequency is maximum in December, their intensity increases from October to March and they last between 1 and 10 days, with the longest events occurring in January.

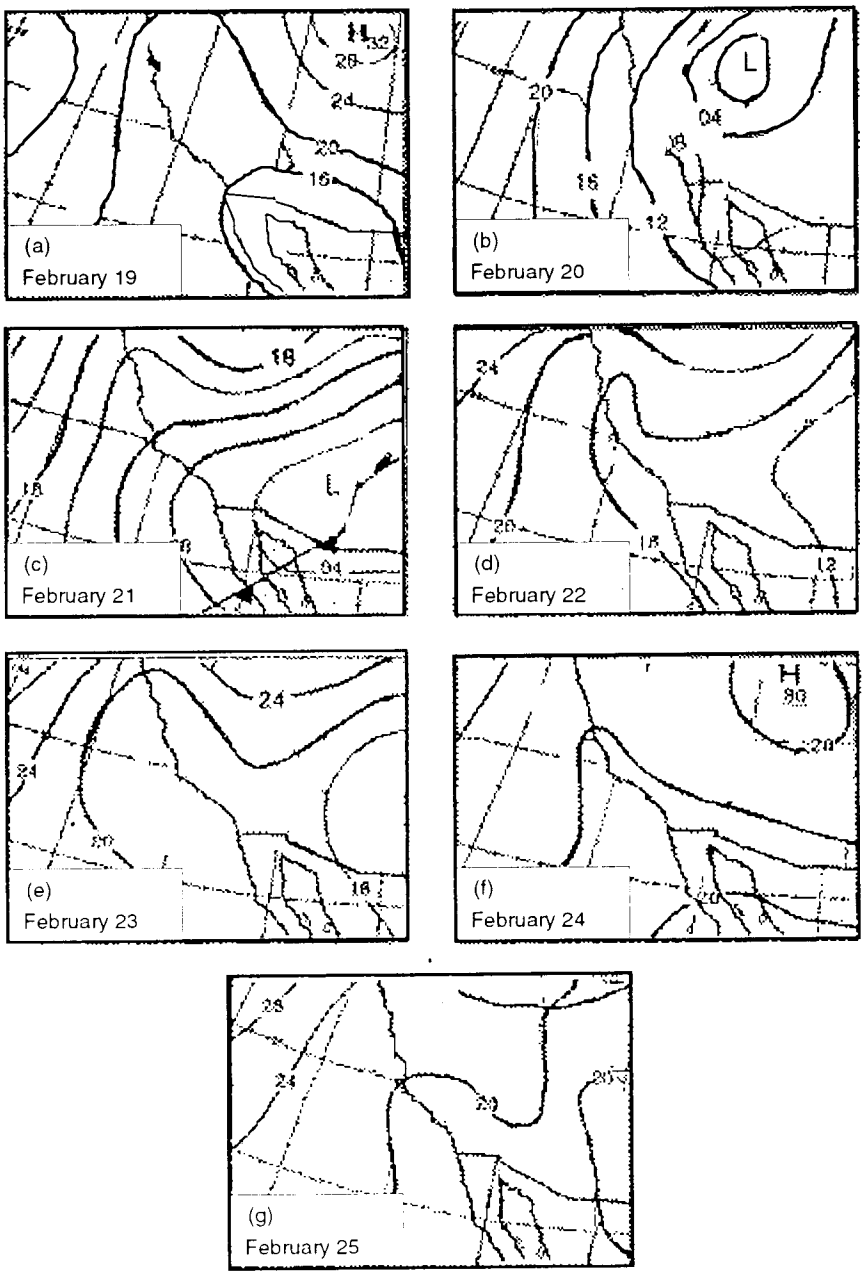


Figure 4. Surface pressure maps from February 19 to 25, 1985, showing the succesion of high and low pressure systems affecting the Northern Gulf of California in autumn-winter. Adapted from National Weather Service.

Table III suggests that during the autumn the NGC is subject to more and longer-lasting but less intense events than in winter. This fact could reflect the southward winter migration of the tropical-extratropical boundary, which brings more frequent disturbances to the latitude of the NGC. The direction of the wind during the winter events is predominantly from the NW, but near the end of the winter it shifts to the N or NE; this suggests that at the beginning of autumn

the NGC is affected mainly by oceanic air masses (from the Pacific) and at the end of winter it is affected mainly by continental air masses. We shall see below that the monthly data shows the same pattern of the wind direction, and also that there are detectable interannual differences.

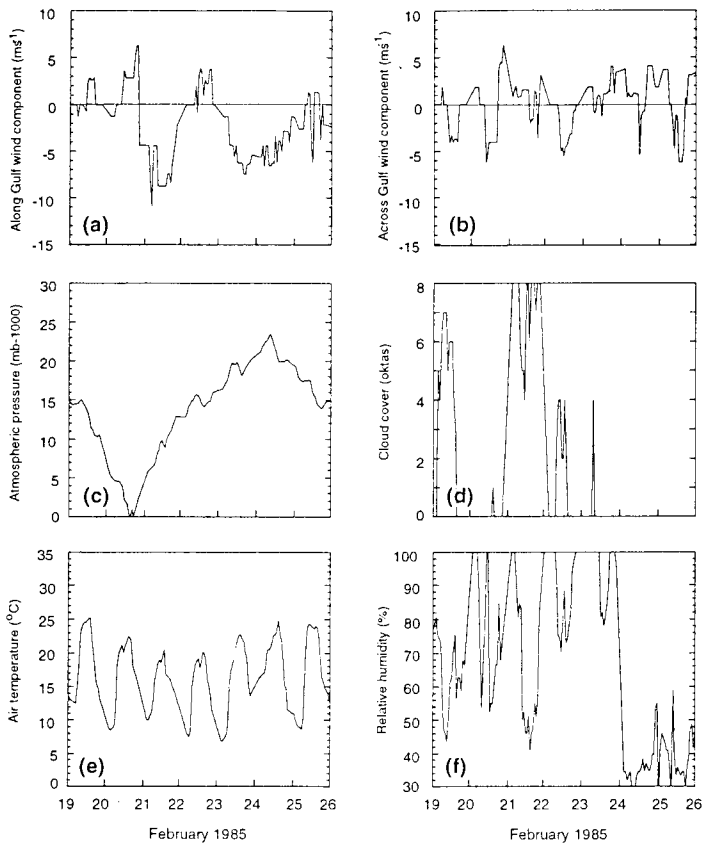


Figure 5. Meteorological data from San Felipe for the same days as in Fig. 4, February 19 to 25, 1985.

Table III. Average characteristics of the "intense wind events".

| Month | No. events | duration in days | Wind speed | Direction |
|---|---|---|---|---|
| October | 3.8 | 2.1 | 5.3 | NW |
| November | 5.2 | 3.7 | 5.1 | NW |
| December | 5.6 | 3.1 | 4.8 | NW |
| January | 4.0 | 3.5 | 8.1 | NW |
| February | 3.2 | 1.0 | 8.1 | NE |
| March | 1.2 | 1.1 | 9.1 | NE |

### *(b) Seasonal and interannual variations*

In the monthly-averaged data (Fig. 6), the winter portion of the seasonal signal of some of the variables is evident, as well as interannual anomalies, the latter especially in humidity and wind.

The following are the statistically significant differences encountered in the data, as revealed by Analysis of Variance (ANOVA). Of the five autumn-winter periods, 1982/83 and 1986/87 showed statistically different relative humidities. During 1982/83 relative humidity and wind speed were the highest. Relative humidity in 1986/87 was the lowest, while the wind was near to the long-term average (1982/83 to 1986/87). Both 1982/83 and 1986/87 were ENSO years (Krueger, 1983; Chen, 1983; Bergman, 1987; Kousky, 1987), it is therefore remarkable that the two periods show anomalies in humidity and in the across-gulf wind component, but of opposite sign (Figs. 6b, and 6e).

Air temperature (Fig. 6a) is lowest in December, the interannual variability is largest in December and January, but the short-term variability (as given by $\sigma$) is such that the monthly temperature in the different years do not differ statistically.

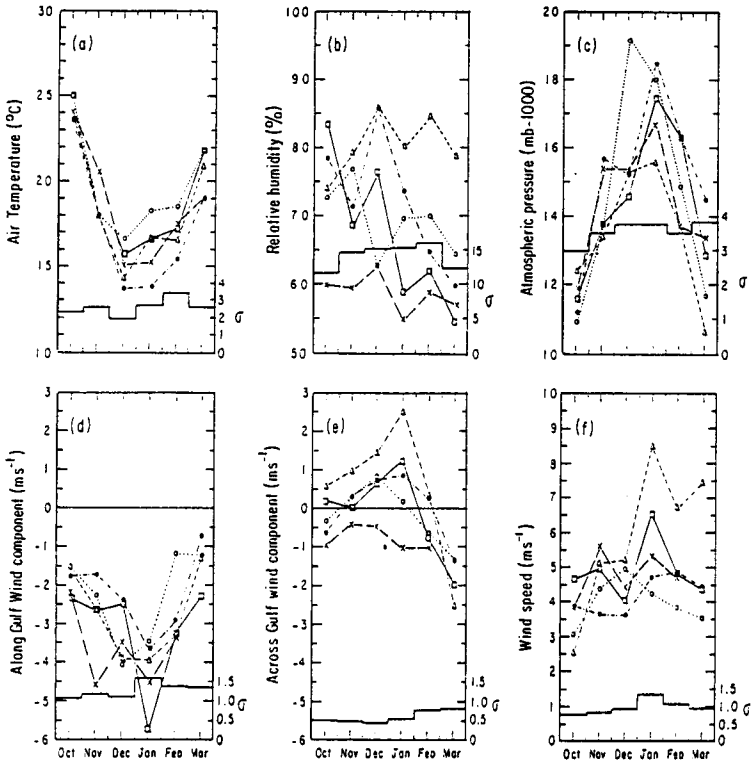


Figure 6. Monthly means of the meteorological data from San Felipe, coded for the the autumn-winter periods: open triangles, 1982/83; open squares, 1983/84; solid circles, 1984/85; open circles, 1985/86; crosses, 1986/87.The solid line without symbol is the mean standard deviation.

Relative humidity (Fig. 6b) suggests, on the one hand a decreasing trend between October and March with two relative maxima (in December and February) for the periods 83/84, and 85/86, and on the other, significant anomalies: in 82/83 humidity seems to be the highest and in 86/87 the lowest.

Atmospheric pressure (Fig. 6c) has a maximum in January (except 85/86), reflecting the seasonality of the pressure centers systems that affect the NGC. The tropical-subtropical atmospheric boundary is at its southernmost portion in December, and the frequent passage of fronts

is revealed by the increased standard deviations of most variables between October and January. Thus the monthly averages and their mean standard deviation suggest that the atmosphere over the NGC passes from a more or less homogeneous, warm and moist condition in October, to a frequently perturbed one (due to the presence of weather fronts) from December. Apart from the lower insolation, air temperature also drops (Fig. 6a) because of the frequent invasions of dry and cold intense NW wind, as the presence of high pressure systems becomes dominant.

Cloud cover (not shown) has a maximum in December, but the variability is much too large to establish a pattern with confidence.

The components of the wind (Figs. 6d and 6e) present a clear seasonal pattern. The along-gulf component is always from the NW and has a maximum in January (Fig. 6d). The across-gulf component has a maximum from the peninsula in December-January and a maximum from the continent in March (Fig 6e). The combination of the components produce, in the average, two wind speed maxima, in November and January (Fig. 6f). At the beginning of the 1982/83 period, the wind speed (Fig. 6f) was the lowest of all but from January it became the highest.

It is now possible to interpret the behavior of relative humidity (Fig. 6b) with the aid of the cross-gulf component of the wind (Fig. 6e): by the end of winter (March), the cross-gulf component has its highest magnitude and is from the continent, it therefore brings dryer air than during autumn.

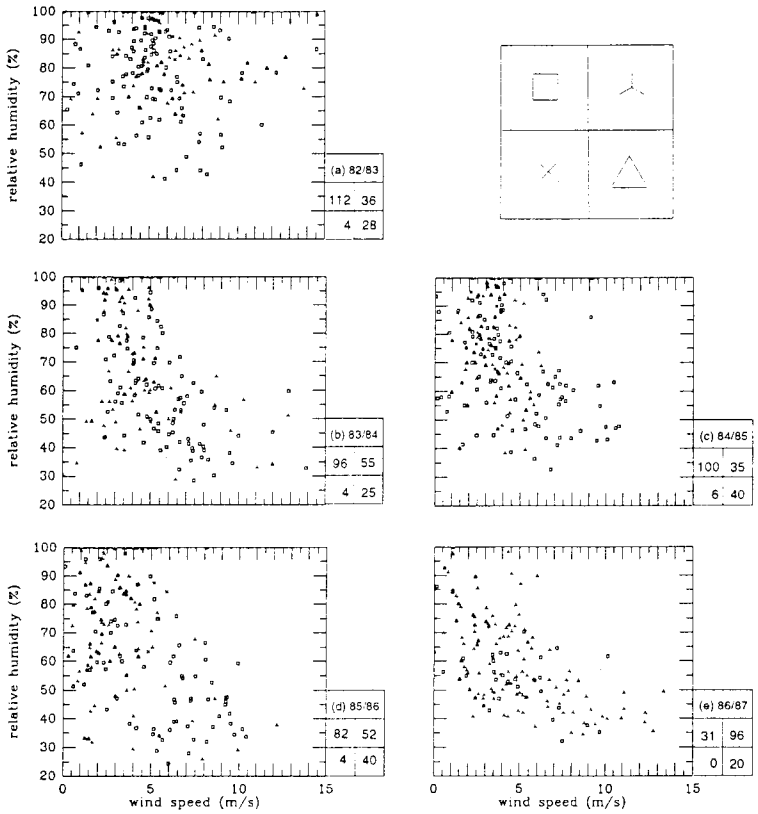


Figure 7. Wind speed versus humidity dispersion diagram. Daily data were used, and the direction of the wind is coded for the quadrant where the wind came for, according to the diagram in the top right corner. The small table on the bottom right of each figure indicates the autumn-winter period involved, and the number of days that the wind blew from the corresponding quadrant.

The interannual anomalies in relative humidity, pointed out before, seem to have a similar explanation. The period 82/83 had the highest humidity because the across-gulf component of the wind was the highest and from the peninsula. In contrast 86/87 had the lowest humidity because the across-gulf component of the wind was quite anomalous, being from the mainland throughout the autumn-winter of 86/87.

The close relationship between relative humidity and wind direction (which indicates the area of origin of the air masses carried by the wind), both in short and interannual time scales, is well illustrated by relative humidity vs. wind speed dispersion diagrams, constructed from daily-averaged data and coded for the quadrant of the wind direction (Fig. 7). With the exception of 1982/83, there is a clear inverse relationship for all years, that is, the strongest winds tend to have low humidities, and to be from the NW quadrant. High humidities occur at low wind speeds, and can be from any quadrant; however, most days with wind from the SE have high humidity. The behavior in 1986/87 seems closer to that of the other three periods, but this is the only period when the number of days with wind from the NE quadrant exceeded those from the NW quadrant, and humidity is lower than in all other periods; indeed there are very few days with humidity > 80%. The number of days with wind from the SW quadrant is negligible.

## 5. Model results

The model (equation 6) was run for each of the autumn-winter periods, always starting with the climatological water temperature of September 30 (equations 1 and 2). Runs were made for water columns of 30 m and 75 m; however, since the results lead to similar conclusions, in the interest of brevity, only the results for the 30 m water column are presented.

### *(a) Temperature*

The temperature of the 30 m water column predicted for all the autumn-winter periods is shown in Figure 8, together with the observed climatological mean $< T_{so} >_{30}$ (thick solid line, calculated from equation 1). The predicted series show (a) the seasonal pattern of sustained cooling until the end of February, (b) short-term fluctuations associated to the weather (these are dampened in the 75 m model, not shown), and (c) interannual anomalies. These anomalies are most noticeable around the time of the minimum temperature (21-28 February), with differences of $\sim 3^{\circ}$C between $< T_{so} >_{30}$ and $T_s$ 86/87. The monthly averages (Table IV) show that the largest differences (average $\sim 1.4^{\circ}$C) occur in October and December.

The anomalous meteorological conditions in the years 82/83 and 86/87 have a substantial effect in the predicted temperature (as it will be shown later). The lowest water temperatures occurred in 1986/87, when humidity was lowest. Although less marked, in 1982/83, when the humidity was higher than usual (and despite the wind being the strongest), the water temperature was higher than the mean.

It is of course limiting that the model was started with the same initial conditions for all the years; it is reasonable to expect the meteorological interannual variability to affect all the seasonal cycle. A study of that, however, is beyond the scope of this work, which is focused on the effect of meteorological variability upon the surface heat loss by the gulf.

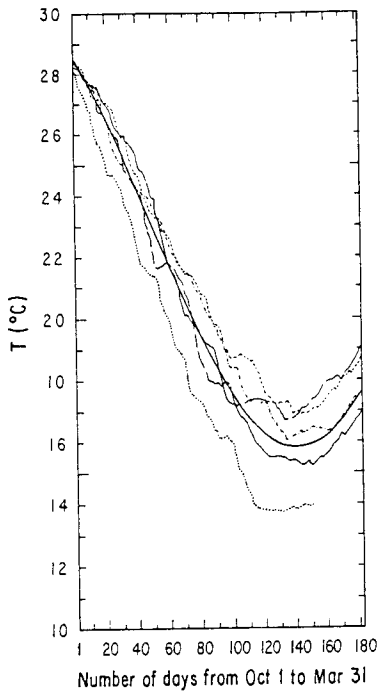


Figure 8. Temperature of a 30 m well mixed water column in the Northern Gulf of California. The thick solid line represents the daily data obtained form an adjusted yearly signal to the monthly mean of the observations (equation 1). The coded traces are the temperatures modeled with equation 6 by using the meteorological data of the different autumn-winter periods: 1982/83, short dash; 1983/84, thin solid; 1984/85, dot-dash; 1985/86, long dash; 1986/87, dotted.

**Table IV. Observed and predicted mean monthly sea surface temperature (°C) for a 30 m water column.**

| h=30m | Oct | Nov | Dec | Jan | Feb | Mar |
|---|---|---|---|---|---|---|
| $\langle T_{s0} \rangle_{30}$ | 28.2 | 23.1 | 18.3 | 16.8 | 16.6 | 17.0 |
| $\langle T_{sp} \rangle_{30}$ | 26.8 | 23.3 | 19.7 | 17.0 | 15.9 | 17.2 |
| $\Delta\langle T_s \rangle_{30}$ | +1.4 | -0.2 | -1.4 | -0.2 | +0.7 | -0.2 |

### *(b) Surface heat flux*

The net surface heat flux (Qf calculated by the model for each autumn-winter period (Fig. 9)) presents a series of episodes during which $Q_f < 0$. Most of the $Q_f < 0$ episodes are associated with the meteorological events of strong winds and low relative humidity described before, although the $Q_f < 0$ episodes seem extend beyond the strong wind events. The $Q_f < 0$ episodes last between 1 and 15 days, the longest occurring between November and January (Table III). From October to January, the episodes with $Q_f < 0$ are due mainly to NW winds, while starting in February, heat loss is caused by NE winds. About 67% of the heat loss events occur under NW winds (Tables III and V).

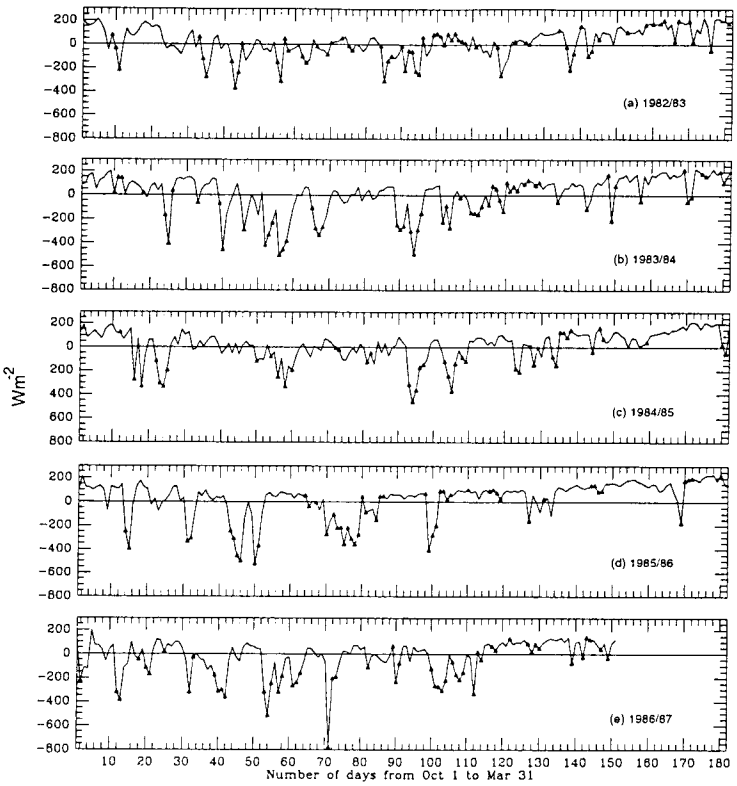


Figure 9. Net surface heat flux calculated using the modeled temperature for a 30 m water column (Figure 8) and the corresponding meteorological data. The triangles mark the the days when intense NW wind events occured.

Table V. Number of $Q_f < 0$ events, total and those from the dominant wind direction (30 m water column).

| h=30m | No. | NW | NE | Other |
|---|---|---|---|---|
| 82/83 | 26 | 22 | 3 | 1 |
| 83/84 | 24 | 20 | 4 | 0 |
| 84/85 | 25 | 20 | 5 | 0 |
| 85/86 | 17 | 11 | 5 | 1 |
| 86/87 | 22 | 9 | 12 | 1 |

On average, the heat lost during events lasting 1 to 7 days is about $44 \times 106$ Jm$^{-2}$, equivalent to a 0.63°C cooling of the 30 m water column. In events 8 to 15 days long, approximately $198 \times 10^6$ Jm$^{-2}$ are lost, equivalent to a cooling of 1.87°C.

In order to quantify the relative importance of the different heat fluxes to the heat loss, $Q_l \equiv Q_e + Q_b + Q_h$ (if $Q_h < 0$), an average value of each term on the right hand side of equation (7) was obtained for each month, using the daily data for the respective month of all the years sampled. This was done in two ways: using all the days (Fig. 10a), and using only the days when $Q_f < 0$ (Fig. 10b). From Figure 10 it is clear that the latent heat ($Q_e$) flux is the most important contributor to the loss of heat from the NGC, both in the mean and during the events.

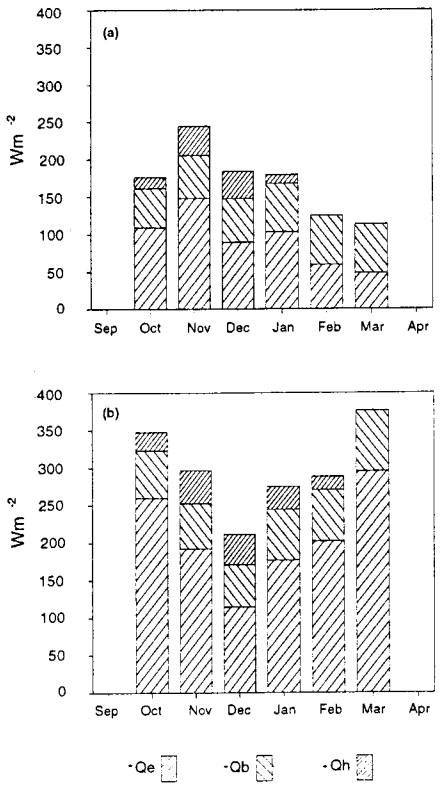


Figure 10. Composition of the ensemble monthly average surface heat loss $Q_l \equiv Q_e + Q_b + Q_h$ ($Q_h < 0$), made with: (a) all the daily values, (b) using only the days when there was a net heat loss ($Q_l < 0$).

In the monthly mean, Qe is the main cooling agent (Fig. 10a) for most of autumn-winter, the exception being February and March, when long-wave radiation ($Q_b$) is as important as $Q_e$; however, their combined effect in those two months is the lowest of the season. In those months, $Q_h > 0$. The overall relative importance of the different fluxes to $Q_l$ is: $Q_e$ between 49% and 62%; $Q_b$ between 24% and 66%; $Q_h$ between 0% and 20%.

There are some details in Figure 10a that deserve explanation in terms of the description of the meteorology made in relation to Figure 6 (or its average, Fig. 11) and the seasonal behavior of the SST (Fig. 8). Although the lowest relative humidity occurs in February and March, $Q_e$ has relative maxima in November and January. The reason for this is that the progressively lower SST dampens $Q_e$. In November, when SST is relatively high ($\sim$22°C, Fig. 8), the coincidence of a maximum in wind speed and a minimum in relative humidity (Fig. 6b and 6f or 11a and 11b) produce the first maximum in $Q_e$ (Nov., Fig. 10a). In January, these conditions are present again (indeed more marked) but the SST has cooled by about 5°C, which causes the second maximum Qe (Jan., Fig. 10a) to be lower than the first. In February and March, when relative humidity is the lowest (Fig. 11a), the relatively weaker winds (Fig. 11b) and (to a larger degree) the lower SST produce the lowest $Q_e$ (February and March, Fig. 10a).

$Q_b$ varies very little (Fig. 10a); this is because of the opposing effects of decreasing SST and relative humidity. The sensible heat flux ($Q_h$, Fig. 10a), which depends mainly on the wind speed and on the air-sea temperature difference, is maximum in November (Fig. 10a), when a maximum in wind speed (Fig. 11b) coincides with a relatively high air-sea temperature

difference. In December $Q_h$ is as large as in November (Fig. 10a), despite a lower wind speed, because the air-sea temperature difference is larger. Although in January the wind speed is maximum, $Q_h$ is lower than in the previous months because the temperature difference is smaller. In February and March, the sea surface is cooler than the air, which produces positive $Q_h$.

During the days when $Q_f < 0$ (Fig. 10b), $Q_l$ is dominated by $Q_e$, with $Q_b$ again being the second contributor. The relative importance of the heat losses when $Q_f < 0$ is: $Q_e$ between 54% and 85%; $Q_b$ between 18% and 27%; $Q_h$ between 0% and 27%. In fact, $Q_h$ does not contribute to $Q_l$ in March because the SST is lower than air temperature. The largest heat loss during events occurs in October and March (Fig. 10b), in contrast with Figure 10a which shows a maximum $Q_l$ in November. This is because winds are strongest and humidity is lowest during the events that occur in October and March (Fig. 11).

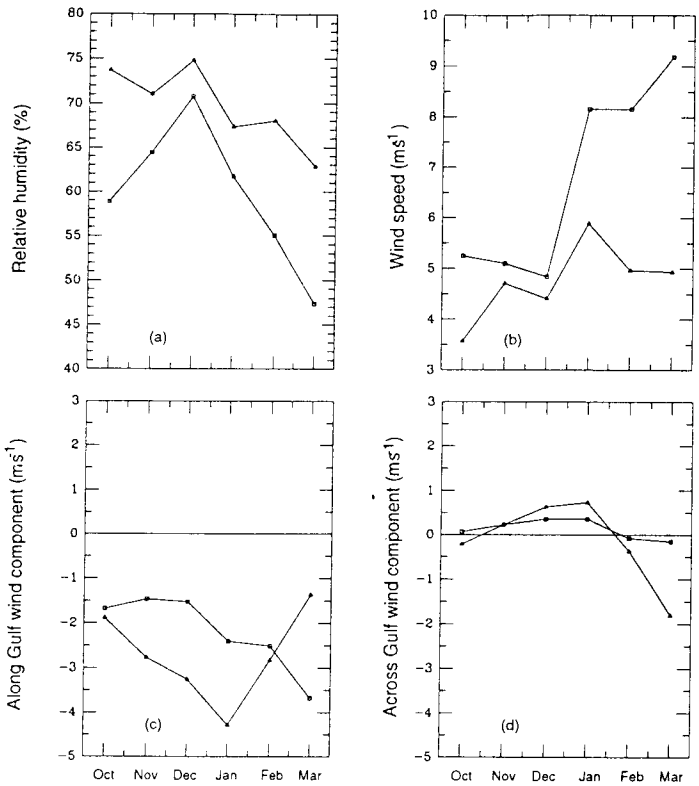


Figure 11. Ensemble monthly averages of the meteorological variables that control heat loss: (a) relative humidity, (b) wind speed, (c) along-gulf component, (d) across-gulf component. Triangles: using all the daily data. Squares: using data from the days when there was a net heat loss ($Q_f < 0$).

### *(c) Interannual variations*

The interannual variation of $Q_f$ is large, as shown by the monthly values of $Q_f$ for the various years (Fig. 12). For instance, the meteorological conditions in 1986/87 produced net heat loss from October to January, while in 1985/86 $Q_f$ was negative only in November and December.

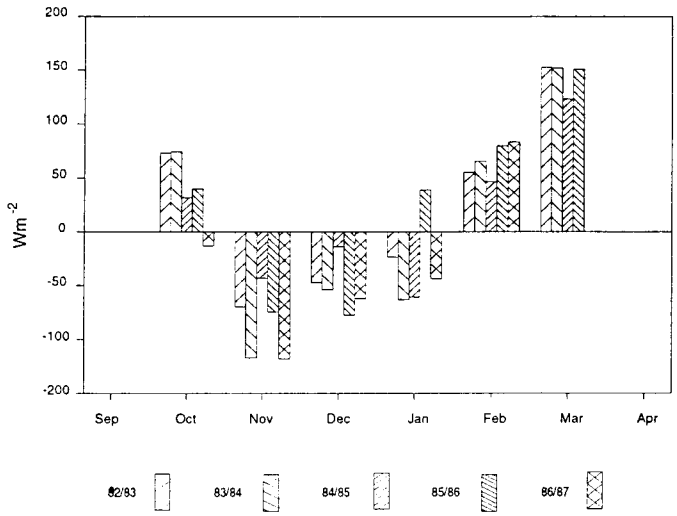


Figure 12. Monthly mean net surface heat flux ($Q_t$) for the autumn-winter periods of 1982/83 to 1986/87

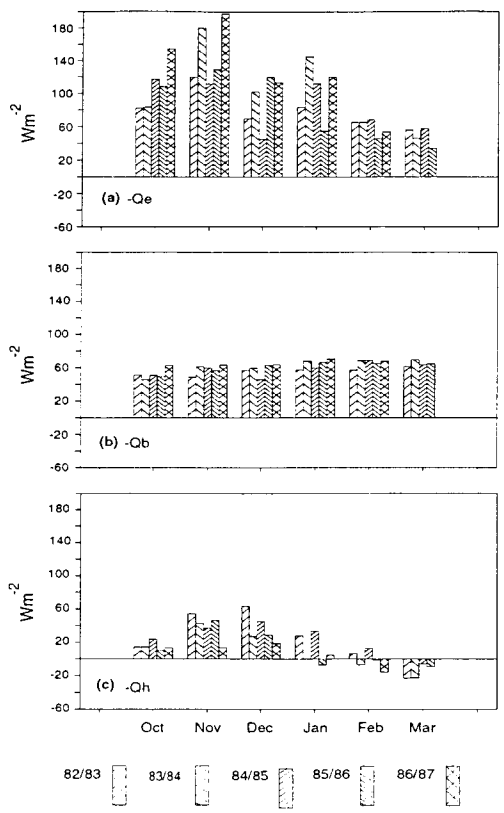


Figure 13. Surface heat losses [(a) $Q_e$, (b) $Q_b$, (c) $Q_h$] for the autumn-winter periods of 1982/83 to 1986/87.

The only October-February average $Q_f$ (no data for March 1987) with small heat gain by the sea, was 1985/86 ($Q_f = 1.34$ Wm$^{-2}$). The more normal periods were 1983/84 ($Q_f = -18.66$ Wm$^{-2}$) and 1984/85 ($Q_f = -7.78$ Wm$^{-2}$). The lowest net heat loss, besides 1985/86, occurred in 1982/83 ($Q_f = -2.31$ Wm$^{-2}$), and the largest in 1986/87 ($Q_f = -30.56$ Wm$^{-2}$); as noted before, these were ENSO years, and were the ones with the the highest and lowest humidities, respectively (Fig. 6b).

The interannual variability in $Q_f$ (Fig. 12) can be traced to that of the individual components of heat loss (Fig. 13), and thence to that of the meteorological variables (Fig. 6). In October 1986, which is the only October when $Q_f < 0$, $Q_e$ and $Q_b$ are larger than for the same month in the other years (Figs. 13a and 13b), due to the extremely low relative humidity and the relatively high wind speed (Figs. 6b and 6f). In the following month (November 1986), this behavior became more marked in $Q_e$, while $Q_b$ remained unchanged because the air-sea temperature contrast had diminished; still $Q_f$ is one of the lowest for November. The only January with a net heat gain ($Q_f > 0$) is that of 1986 (Fig. 12), which is the month with the lowest $Q_e$ of the five autumn-winter periods analyzed (Fig. 13a), and caused 1985/86 to be the only autumn-winter period with average $Q_f > 0$; the reason for this anomaly can be traced back to relatively high humidity and low wind speed in January 1986 (Figs. 6b and 6f).

In the autumn-winter average, 1982/83 and 1986/87 show substantial differences in the heat losses (Fig. 13): in 1982/83 $Q_e$ and $Q_b$ were relatively low, contributing with 49% and 31% of $Q_l$ respectively, while $Q_h$ is relatively high (19%). By contrast, in 1986/87 $Q_e$ and $Q_b$ are relatively high, 64% and 33%, respectively, while $Q_h$ is only 3%. These differences are clearly due to the meteorological variability, as discussed before.

## 6. Discussion

*Data*

As Lavín and Organista (1988) pointed out, the data from Puerto Peñasco (Fig. 1), seem to be more representative of conditions offshore than those from San Felipe, but the data from San Felipe were sampled more consistently. In order to improve somewhat the representativeness of the data to conditions offshore, and based on the homogeneity of the marine layer over the NGC (Merrifield and Winant 1989; Paden *et al.*, 1993; Badan-Dangon *et al.*, 1991), the "calibration" described in the Data section was performed; limited as this may be, we believe it is an improvement over using data based over land.

In comparison with the 1984/85 Isla Tortuga data, which has been proposed to be representative of meteorological conditions offshore (Badan-Dangon *et al.*, 1991; Paden *et al.*, 1993), the monthly averages of the calibrated data presents higher humidity (34% higher in December), and lower wind speeds (maximum difference 1.5 ms$^{-1}$, also in December). The maximum daily mean wind speed during NW winds agree fairly well, with 18 ms$^{-1}$ for this data vs. 15 ms$^{-1}$ reported by Merrifield and Winant (1989). Apart from the shortcomings of the coastal data, some of the differences are probably due to the fact that San Felipe and Isla Tortuga are located in two different meteorological regimes (Hasting and Turner, 1965; Reyes and Rojo, 1985). For instance, during the invasion (in February 1985) of the NGC by a low pressure center (Reyes, 1993), the wind in San Felipe and Puerto Peñasco was from the NW, while in Isla Tortuga it was from the SE (Merrifield *et al.*, 1987). The description of the synoptic meteorological conditions and their reflection on the San Felipe data is not affected by this problem. The heat flux calculations are more sensitive to the quality and representativeness of the data used, but at least the relative

importance of the different components of $Q_l$ can be obtained with confidence. The numerical values will need to be reviewed whith offshore time series of meteorological conditions.

*Meteorology*

A description has been given of the synoptic conditions that gives rise to NW wind events during winter. Although it is known that there is a large variability in the trajectories followed by the centers of high and low pressure, it was possible to establish the basic effects of these movements upon the local meteorology and herefore the surface heat fluxes in the NGC. Since the NGC lies in the tropical-subtropical boundary, an explanation of the behavior of the atmosphere in autumn-winter must be based on the North-South displacement of the centers of high and low pressure that dominate the meteorology of this region. Roden (1958) noted the relationship among the winds, the rainy season and the position of the far southeast position of the Mexican Low during winter, and Hastings and Turner (1965) explaining the Southward migration of the precipitation maximum in the western USA and NW of Mexico as winter progresses, indicate that the large-scale winter conditions are characterized by the weakening and migration to the SE of the Pacific High, and by the corresponding definition and intensification of the Aleutian Low (Fig. 2b); the reverse behavior being observed in spring.

The observed veering of the wind to the NE and the relative humidity decrease at the end of winter are consistent with a displacement to the NW of the boundary between the Pacific Anticyclone and the Mexican Low, as suggested by the typical sea level distribution of pressure for January (Figs. 2 and 6c). Thus, autumn and winter conditions are very well identified by the wind regime: NW winds relatively humid in autumn, dry NE winds in winter.

*ENSO*

A remarkable disparity of meteorological conditions was found between the two ENSO years that were sampled. While the autumn-winter of 1982/83 was the most humid, that of 1986/87 was the driest. The explanation of this illustrates how the dominant wind direction determines the origin of the air mases being carried to the NGC. The main air masses that invade the NGC are the Polar Continental air mass and the Maritime Polar (or Transition) Air mass. The later air mass does not have well defined characteristics; it "usually form through consenescence of air from the neighboring sources" (Petterssen, 1940, p.162), that is, from the Arctic, Polar Continental and Tropical Maritime air masses. The cause of the high relative humidity during 1982/83 can be explained by a larger influence of Tropical Maritime Air, caused by an abnormal propagation of warm water to the Pacific coast of the USA (Wyrtki, 1985). This warm water should have moved the Mexican Low to the NE of its winter normal position (resembling that of the summer normal position), making it easier for cyclonic cells to migrate over the northeast edge of the Pacific High to invade the continent, thus bringing higher humidity. A possible explanation of the conditions in 1986/87, when NE wind dominated, would be the opposite condition; if the warm water is not sufficiently displaced northward, the Mexican Low sets further south, and the High establishes itself close to the NGC, hindering the movement of the migratory Lows toward the continent, facilitating the advection of dry continental air. These hypothesis about the transportation of humid or dry to the NGC during ENSO require further research.

*Heat flux calculations*

Table VI compares the monthly values of $Q_f$ of this work and those of Lavin and Organista (1988) as revised by Castro *et al.* (1994). In the present work, higher heat loss and a longer

cooling period are obtained (November-January vs. November-December). This may be due in part to the different data sets and to the algorithm used to convert data collected at San Felipe to conditions offshore. Although the actual values of $Q_f$ may not be very accurate, the relative importance of the different heat fluxes, and the dominant effect of the strong wind events is clearly established. Most of the major $Q_f < 0$ events occur in November, when the wind speed has a relative maximum and the air-sea temperature contrast is highest. This is consistent with the findings of other heat-flux studies in the NGC (Organista, 1987; Paden, 1991; Castro *et al.*, 1994), and with that of Zhao and McBean (1986) in the California Current, who attribute the maximum to more frequent westerly winds, which rise the humidity and the temperature difference between the atmosphere and the ocean.

Table VI. Monthly net heat flux according to this work and Lavin and Organista (1988).

| h=30m | Oct | Nov | Dec | Jan | Feb | Mar |
|---|---|---|---|---|---|---|
| This work | 41.3 | -84.4 | -50.7 | -30.3 | 66.2 | 144.7 |
| (L&O)coast | 17.4 | -19.0 | -16.8 | 22.6 | 66.6 | 98.3 |
| (L&O)off-shore | 03.0 | -43.5 | -42.9 | 5.3 | 44.8 | 113.5 |

The value of the largest $Q_f < 0$ peaks agree with previous studies in the NGC (Organista, 1987; Figueroa and Palacios, 1991) and with those calculated by Camp and Elsberry (1978) for the Eastern Pacific. The largest peak occurred in November 1986, and its value is comparable with $Q_f$ for the eastern Mediterranean reported by Bunker (1972) and by Leaman and Schott (1991).

## 7. Conclusions

Because during the autumn-winter period the boundary between the tropical and subtropical atmospheric circulation regimes pass over the NGC, this area is subjected to meteorological conditions that cause intense heat loss. In addition, these conditions lead to a marked interannual variability.

Most of the heat losses occur during high wind speed events ($\sim$7 ms$^{-1}$, mostly from the NW) and low relative humidity ($\sim$56%). During these events, the NGC losses more than 2/3 of the total heat lost from October to March. The largest heat loss per event occur in October and March.

The latent heat flux ($Q_e$) is the most important contributor (62%) to the loss of heat by the NGC, both in the mean and during the events (Fig. 12). The second most important heat loss mechanism is long wave radiation. The monthly-mean latent heat flux presents two relative maxima, in November and January.

Interannual variability was detected in the meteorological data, and it was found to have an important effect upon the heat losses. In the autumn-winter of 1982/83 mean humidity was the highest (63%), while in 1986/87 it was the lowest (43%). A clear relationship exists between these anomalies and the direction of the wind: NW in 1982/83 and NE in 1986/87. As a consequence, 1982/83 had the lowest latent and long-wave heat fluxes and the highest sensible heat flux. 1986/87 showed the opposite behavior.

The main results of this work are: (i) The description of synoptic meteorological conditions that cause the heat loss events, (ii) The detection and description of anomalous conditions during ENSO and their effect upon heat loss, (iii) The dominant effect of the strong wind events and the relative importance of the different heat losses. Although we believe that these results can withstand the shortcomings of the data, it is clearly desirable that efforts be made to obtain time series of offshore meteorological conditions. This is being done at present.

## Acknowledgements

This research was supported by Consejo Nacional de Ciencia y Tecnología (CONACyT grant 3209-T) and by CICESE's budget from the Secretaría de Educación Pública (México). A. C. R. held a CONACyT postgraduate scholarship. We thank the Servicio Meteorológico Nacional for making their data available.

## REFERENCES

Argote, M. L., A. Amador, M. F. Lavín and J. R. Hunter, 1995. Tidal dissipation and stratification in the Gulf of California. *J. Geophys. Res.*

Badan-Dangon, A., C. Dorman, M. Merrifield, and C. Winant, 1991. The lower atmosphere over the Gulf of California. *J. Geophys. Res.*, **96(C9)**, 16877-16896.

Bailey, H. P., 1975. Weather of Southern California. University of California Press. 87 pp.

Bergman, K. H., 1987. The global climate of September-November 1986: A moderate ENSO Warming Develops in the tropical Pacific. *Month. Wea. Rev.*, **115**, 2524-2541.

Bunker, A. F., 1972. Wintertime Interactions of the Atmosphere with the Mediterranean Sea. *J. Phys. Oceanogr.*, **2**, 225-238.

Bray, N., 1988. Water mass formation in the Gulf of California. *J. Geophys. Res.*, **93**, 9223-9240.

Camp, N. T and Elsberry R. L., 1978. Oceanic Thermal Response to Strong Atmospheric Forcing. II. The Role of One-Dimensional Processes. *J. Phys. Ocean.*, **8**, 215-223.

Castro, R., M. F. Lavín and P. Ripa, 1994. Seasonal Heat Balance in the Gulf of California. *J. Geophys. Res.*, **99(C2)**, 3243-3261.

Chen, W. Y., 1983. The climate of Spring 1983 - A Season with Persistent Global Anomalies Associated with El Niño. *Month. Wea. Rev.*, **111**, 2371-2384.

Douglas, M. W., 1995. The Summertime Low-level Jet over the Gulf of California. *Month. Wea. Rev.*, **123**, 2334-2347.

Figueroa, J. M. and M. R. Palacios, 1991. Surface heat and momentum fluxes in the Gulf of California. *Ciencias Marinas*, **17(2)**, 109-149.

Franklin, B. S. and J. O. Blanton, 1984. The Use of Land and Sea Based Wind Data in a Simple Circulation Model. *JPO*, **14**, 193-197.

García, E. and A. P. Mosiño, 1966-67. Los Climas de Baja California. (Memoria) Decenio Hidrológico Internacional. UNAM.

Hales, J. E., 1972. Surges of maritime tropical air northward over the Gulf of California. *Month. Wea. Rev.*, **100**, 298-306

Hastings, J. R. and R. M. Turner, 1965. Seasonal precipitation regimes in Baja California Mexico. *Geografiska Annaler*, **47A**.4.

Igmanson, D. E. and W. J. Wallace, 1985. Oceanography an Introduction, 3rd. Edition, Wadsworth Publishing Company, Belmont California. 530 pp.

Ives, R. L., 1962. The "Pestiferous Winds" of the Upper Gulf of California. *Weatherwise*, **15** (5), 196-201.

Kousky, V. E., 1987. The Global climate for December 1986-February 1987: El Niño Returns to the Tropical Pacific. *Month. Wea. Rev.*, **115**, 2822-2838.

Krueger, A. F., 1983. The climate of Autumn 1982 -With a discussion of the major tropical Pacific Anomaly. *Month. Wea. Rev.*, **111**, 1103-1118.

Lavín, M. F. and S. Organista, 1988. Surface heat flux in the Northern Gulf of California. *J. Geophys. Res.*, **93**, 14033-14038.

Leaman, K. D. and F. A Schott, 1991. Hydrographic Structure of the Convection Regime in the Gulf of Lions: Winter 1987. *J. Phys. Oceanogr.*, **21**, 575-598.

Martinez-Sepúlveda, M., 1994. Descripción de la profundidad de la capa mezclada superficial en el Golfo de California. BSc thesis, UABC, Ensenada, Mexico. 48 pp.

Merrifield, M. A., A. Badan-Dangon and C. Winant, 1987. Temporal behavior of lower atmospheric variables over the Gulf of California, 1983-1985: A data report, SIO reference series # 87-6, Scripps Inst. of Oceanogr., La Jolla, Calif. 192 pp.

Merrifield, M. A. and C. Winant, 1989. Shelf Circulation in the Gulf of California: A Description of the Variability. *J. Geophys. Res.*, **94(C12)**, 18133-18160.

Organista, S., 1987. Flujos de calor en el Alto Golfo de California. MSc thesis, CICESE, Ensenada, Mexico. 142 pp.

Paden, C., M. Abbott and C. D. Winant, 1991. Tidal and Atmospheric forcing of the upper ocean in the Gulf of California. 1. Sea Surface Temperature Variability. *J. Geophys. Res.*, **96(C10)**, 18337-18359.

Paden, C., C. D. Winant and M. Abbott, 1993. Tidal and Atmospheric forcing of the upper ocean in the Gulf of California. 2. Surface heat flux. *J. Geophys. Res.*, **98(C11)**, 20091-20103.

Pettersen, S., 1940. Weather Analysis and Forecasting, 1st. Edition, 2nd. impression. McGraw-Hill Book Company, Inc. 503 pp.

Reyes, C. S., L. E. Pavía, P. J. Candela and G. R. Troncoso, 1984. Estudio preliminar de las condiciones meteorológicas y climatológicas alrededor del Golfo de California, 1ra. Parte: Análisis del Viento. *Ciencias Marinas,* **10(2)**, 9-26.

Reyes, C. S. and G. Vogel., 1984. Estudio preliminar de las condiciones meteorológicas y climatológicas alrededor del Golfo de California 2da. Parte: Análisis de los parámetros termodinámicos, *Ciencias Marinas,* **10(2)**, 45-64.

Reyes, C. S. and S. P. Rojo, 1985. Variabilidad de la precipitación en la Península de Baja California. *Revista Geofísica*, **22/23**, 111-128.

Reyes, A. C., 1993. Efectos de las condiciones atmosféricas de otoño e invierno sobre la formación de masas de agua en el Golfo de California. MSc thesis, CICESE, Ensenada, México, 91 pp.

Roden, G. I., 1958. Oceanographic and Meteorological Aspects of the Gulf of California. *Pac. Sci.*, **12** (1), 21-45.

Sorkina, A. I., 1963. Atmospheric Circulation and the Related Wind Fields Over the North Pacific. Gidrometeorologicheskoe Izdatel'stvo (Otdelenie), Moskva. 218 pp.

Sverdrup, H. U., 1941. The Gulf of California. Preliminary discussion of the cruise of the E.W. Scripps in February and March. 1939. 6th Proc. Pac. Sci. Congr., 3: 161- 166.

Wyrtki, K., 1985. Sea Level fluctuations in the Pacific during 1982-1983 El Niño, *Geophys. Res. Lett.*, **12**, 125-128.

Zhao, Y. P., and G. A. McBean, 1986. Annual and Interannual Variability of the North Pacific Ocean-to-Atmosphere Total Heat Transfer. *Atmosphere-Ocean*, **24 (3)**, 265-282.

Zishka, K. M. and P. J. Smith, 1980. The Climatology of Cyclones and Anticyclones over North America and Surrounding Ocean Environs for January and July, 1950-77. *Mon. Wea. Rev.*, **108(4)**: 387-401.